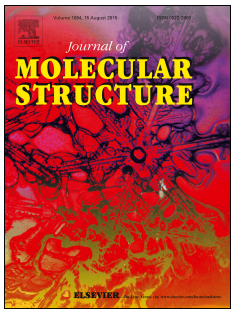

Synthesis, single crystal XRD and CT DNA / BSA binding studies of new paracetamol derivatives

N. Ugin Inba Raj

PII: S0022-2860(20)30235-0

DOI: https://doi.org/10.1016/j.molstruc.2020.127911

Reference: MOLSTR 127911

To appear in: *Journal of Molecular Structure*

Received Date: 27 August 2019

Revised Date: 5 February 2020

Accepted Date: 13 February 2020

Please cite this article as: N. Ugin Inba Raj, Synthesis, single crystal XRD and CT DNA / BSA binding studies of new paracetamol derivatives, *Journal of Molecular Structure* (2020), doi: https://doi.org/10.1016/j.molstruc.2020.127911.

Credit Author Statement

Dr.UGIN INBA RAJ N : Conceptualization, Methodology, Software **,** Data curation, Writing- Original draft preparation, Visualization, Investigation, Supervision, Software, Validation, Writing- Reviewing and Editing

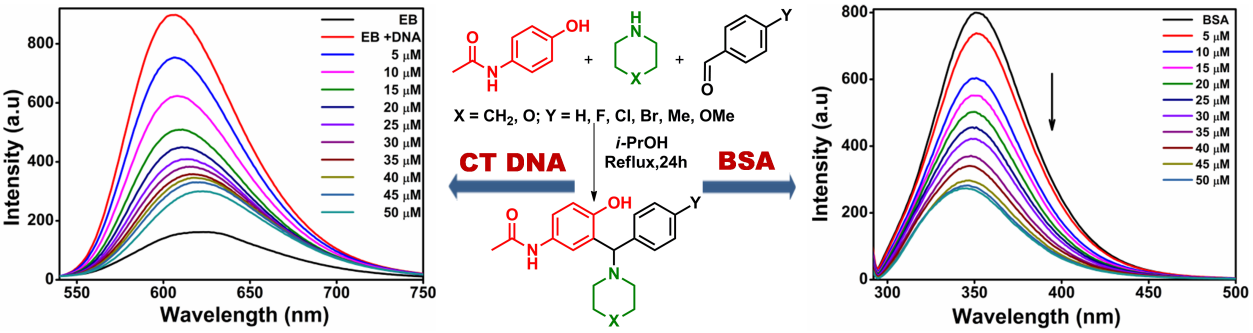

Journal of Molecular Structure
journal homepage: www.elsevier.com/ locate/molstruc

Synthesis, Single Crystal XRD and CT DNA / BSA Binding Studies of new Paracetamol Derivatives

Ugin Inba Raj N
Department of Chemistry, Malankara Catholic College, Mariagiri, Tamil Nadu - 629153, India

ARTICLE INFO

Article history:
Received
Received in revised form
Accepted
Available online

Keywords:
synthesis
Paracetamol
Mannich Base
CT DNA
BSA

ABSTRACT

N-(4-hydroxy-3-(morpholino(phenyl)methyl)phenyl) acetamide and *N*-(4-hydroxy-3-(piperidin-1-yl(phenyl)methyl)phenyl) acetamide derivatives have been synthesized via three component reaction of paracetamol, morpholine/piperidine and benzaldehyde. The reaction afforded these novel paracetamol derivatives in moderate to good yield. The solid state structures of some compounds were examined by X-rays from single crystals .The DNA-binding interactions of the compounds with calf thymus DNA have been studied by UV, visible, emission studies. The results were observed hypochromism with red shift suggesting that compounds interact with CT DNA *via* intercalation. The protein-binding interactions of the compounds with BSA were examined by fluorescence, synchronous fluorescence and UV, visible spectroscopic methods. All the compounds have the ability to bind strongly with BSA and a static quenching mechanism was observed.

1. Introduction

Multicomponent reaction (MCR) is one in which three or more reactants react in one reaction condition and produce a product with substantial portion of all reactants. [1, 2] The organic chemists paid more attention in designing new MCR and enlightening known MCR due to single step reaction with high atom economy and multiple bond forming energy.[3, 4] The MCR is environment friendly process due to reduction in the number of steps, time of labour, energy consumption, cost and isolation of intermediates from product.[5, 6] Several carbon−heteroatom bond and carbon−carbon bond forming reactions have been achieved using MCR in one pot.[7, 8] One such reaction is formation of methylated products through Mannich reaction[9].[10]

The Mannich reaction is most important for producing secondary and tertiary amine derivatives via condensation reaction between active hydrogen compound, amine and non enolizable aldehyde.[11] The obtained amine derivatives are used for synthesizing biologically active compounds, natural products and reactive intermediates.[12, 13] The chiral Mannich bases are important tool for synthesis of pharmaceutical agents.[14] The optically active amino alkylated products act as excellent ligands in asymmetric catalysis.[15]

Worldwide, paracetamol is used as an antipyretic and analgesic.[16] The benzene ring of the paracetamol undergoes electrophilic substitution reaction due to the presence of two activating groups namely, hydroxyl and amide groups. The literature survey reveals that paracetamol and its derivatives are reported as anticancer, antibacterial, antifungal agents and anti-arrhythmic drugs.[17, 18] The amino methylated paracetamol derivatives have been used as intermediates for the synthesis of malarial drugs such as amodiaquine, isoquine and artemisinin etc.[19-21]

Deoxyribonucleic acid (DNA) is a significant biological macromolecule which plays a central role in life processes.[22] It is involved in protein biosynthesis and carries essential genetic information. Nowadays, study of DNA binding interaction provides new architectural motifs with high potential probes for chemical biology and therapeutic agents against many DNA-related diseases.[23, 24] The literature reveals that many small molecules like cisplatin, polyamides, polyimides, octahedral metal complexes and peptide nucleic acid etc bind to DNA.[25-27] Generally, the type of binding with DNA is of fundamental importance to take benefit of the drug- DNA binding.

Serum albumin has been established as the most abundant protein in the circulatory system and serves as a significant medium for transporting several endogenous and exogenous substances.[28, 29] Bovine Serum Albumin (BSA) structurally resembles to human serum albumin (HSA) and so it is being widely used to many of the biological studies. [30] Due to the stability, availability and astonishing binding capacity of serum albumin it acts as a model for drug protein binding interaction and gives the fundamental understanding of dug protein binding interactions.[31]

Previously, the paracetamol was amino methylated using piperidine and formaldehyde (Scheme 1). Generally the rate of Mannich reaction depends on the nucleophilicity of the active hydrogen compound and basicity of the reaction medium.[32]

*Corresponding author. Tel: +91-9994091886; Email: nugin86@gmail.com.

The amino methylation commonly occurs in phenolic Mannich base.[33] But the amino aryl methylation is a difficult process due to the sterically hindered phenyl group.[34] Here we report the novel amino arylated paracetamol derivatives via multicomponent reaction of paracetamol, secondary amine and benzaldehyde (Scheme 2). The reaction was carried out without any catalyst under simple reaction conditions. The CT DNA and BSA binding properties of the compounds were studied using UV, visible and fluorescence spectroscopic studies.

Previous work [20]:

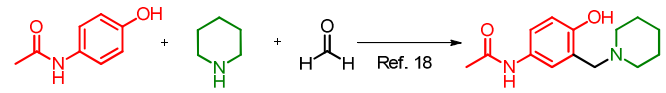

Scheme 1. Synthesis of amino methylated Mannich base.

Present Work

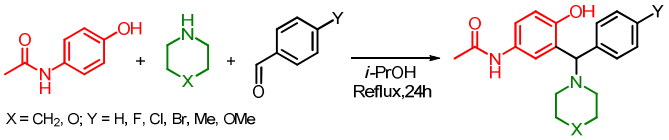

Scheme 2. Synthesis of amino aryl methylated Mannich base.

2. Results and Discussion

2.1. Synthesis

Initial effort was focussed on examining the assembly of paracetamol **3**, piperidine **2** and benzaldehyde **1** and to obtain amino aryl methylated paracetamol. Initially, a mixture of paracetamol **3**, piperidine **2** and benzaldehyde **1** were taken in a mortar and ground well without solvent for 1 h. The reaction did not afford any product (Table 1, entry 1) and the mixture of the above reactants was stirred using methanol as a solvent at room temperature for 48 h and the reaction did not result in any product (Table 1, entry 2). When the mixture of the reactants was refluxed using methanol, the reaction afforded the expected product 4a in 65% yield (Table 1, entry 3). The heating of the reactants in neat condition at 85 ºC afforded the product **4a** but only in 40% yield (Table 1, entry 4).

Table 1. Optimization of reaction conditions in condensation of paracetamol, piperidine and benzaldehyde.

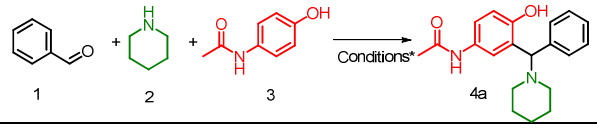

Entry	Solvent	Temperature (^{0}C)	Time (h)	Yield (%)
1	Neat (Grinding)	RT	1	n.d.
2	Methanol	RT	24	n.d.
3	Methanol	65	24	65
4	Neat	85	8	40
5	Ethanol	78	24	68
6	Isopropanol	82	24	72
7	MeCN	80	24	61
8	DMF	85	24	67
9	DMSO	85	24	65
10	Water	85	24	n.d.

Reaction conditions*: 1 (5 mmol), 2 (5 mmol), and 3 (5 mmol) in solvent (15 mL) at the indicated temperature. Yield is tabulated. n.d. = not detected

The compound **4a** is characterized by spectroscopic techniques such as FTIR, ^{1}H NMR, ^{13}C NMR, DEPT-135 and HRMS and the structure was unambiguously confirmed by single crystal XRD (Figure 1).

In order to improve the yield of 4a, the reaction was carried out in various solvents such as ethanol, isopropanol, acetonitrile, DMF, DMSO and water at various heating conditions (Table 1, entry 5-11). The reaction with isopropanol as solvent at reflux condition afforded 4a in 72% yield. Thus entry 6 in Table 1 was found to be the optimized condition for the formation of the amino aryl methylated paracetamol **4a**.

In order to examine the scope of the reaction, the reaction with para-substituted benzaldehydes was carried out and the effect of substitution of aldehyde was studied in the amino aryl methylated paracetamol derivatives **4** (Table 2). Both electron withdrawing groups such as chloro and bromo groups and electron releasing groups such as methyl and methoxy groups in substituted benzaldehydes afforded the corresponding product in moderate to good yield (Table 2, entry 1-5). Benzaldehyde substitution with electron withdrawing groups resulted in good yield compared to electron releasing groups, obviously due to the higher electrophilicity of the electron withdrawing groups substituted in benzaldehyde. The para substituted chloro benzaldehyde afforded the product in high yield 77% (Table 2, entry 2).

Table 2. Scope of Aldehyde.

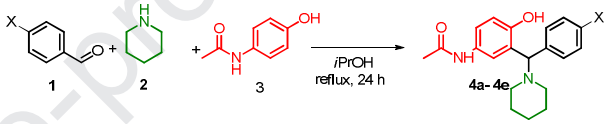

Entry	X	Product	Yield (%)
1	H	4a	72
2	Cl	4b	77
3	Br	4c	73
4	Me	4d	67
5	OMe	4e	64

Reaction conditions: 1 (5 mmol), 2 (5 mmol), and 3 (5mmol) in solvent (15 mL) at the reflux condition. Isolated yield is tabulated.

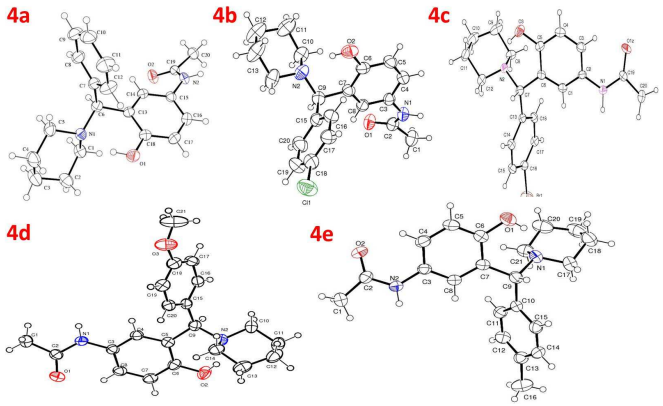

Figure 1: Single crystal XRD of 4a-4e

The reaction scope was further tested by replacing the secondary amine piperidine **2** with morpholine **5**. Interestingly, when the mixture of paracetamol **3**, morpholine **5** and benzaldehyde **3** was refluxed in isopropyl alcohol, it afforded the corresponding amino aryl methylated product **6a** in 74% yield (Table 3, entry 1). The structure of **6a** was characterized by spectroscopic techniques such as FTIR, ^{1}H NMR, ^{13}C NMR, DEPT-135 and HRMS and the structure was confirmed by single crystal XRD (Figure 2).

The reaction is extended to various substituted benzaldehydes and it was found that morpholine afforded the corresponding products (**6a - 6f**) in higher yield (Table 3) compared to piperidine (**4a - 4e**). Similar to piperidine,

morpholine also showed the same substitution effect in the yield of the products (Table 3, entry 1-6).

Table 3. Scope of Aldehyde.

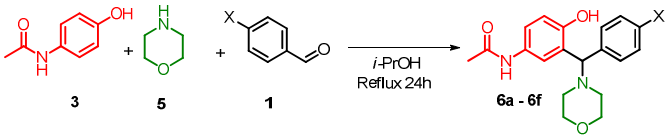

Entry	X	Product	Yield (%)
1	H	6a	74
2	F	6b	80
3	Cl	6c	78
4	Br	6d	77
5	Me	6e	70
6	OMe	6f	67

Reaction conditions: 1 (5 mmol), 2 (5 mmol), and 3(5 mmol) in solvent (15 mL) at the reflux condition. Isolated yield is tabulated.

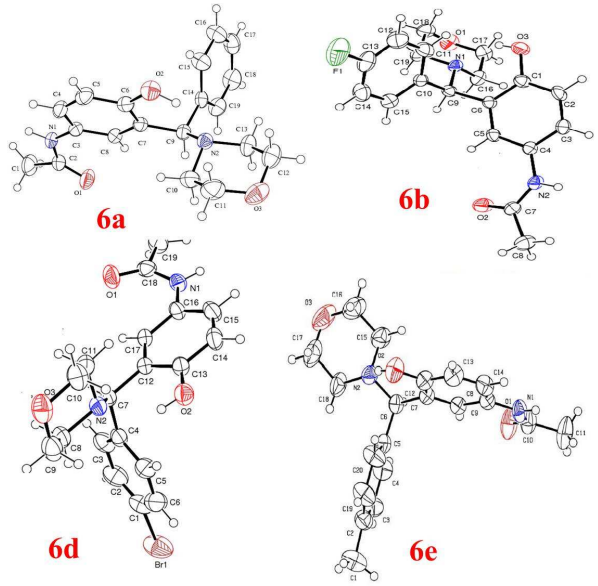

Figure 2: Single crystal XRD of 6a,6b,6d& 6e

2.2. Crystal structure

The X-ray analyses showed that the molecules of all five Mannich bases **4a-4e** had slightly different structures. There is only one molecule in an asymmetric unit cell in all the five Mannich bases. The molecules of these Mannich bases are built up from three five and six-membered rings connected through a methine carbon in the molecule and there not in single plane. The ORTEP diagrams of **4a-4e** are shown in figure 1 and the hydrogen bonds in the structures were listed in table S3.The supramolecular aggregation for the Mannich bases under discussion is simple. Mannich bases **4a-4e** which could form an intermolecular hydrogen bond via O-H…N1. The cyclic five membered motifs were formed for all the compounds and shown in figure S1. The principal motifs in the crystal structures of compounds L1&L2 are constructed by means of N1B-H…O1A and N1A-H…O1B and form a one dimensional linear structure with graph set of R22(16). Inter and intra molecular 3D supramolecular motif structure was shown in figure S2& S4. The formation of the two-dimensional supramolecular structure in the Mannich bases **4c-4e** were readily analysed in terms of the amide as the basic building block. A pair of intermolecular N(2)-H(2)...O(2)#1 and N(2)-H(2)...O(2)#1 hydrogen bonds in Mannich bases **4c-4e** generates a zig zag structure (Figure S3). The best packing view for Mannich bases **4c-4e** is obtained along the b-axis forming a tunnel like structure (S5).

The Mannich bases **6a & 6e** contains only one symmetry independent molecule is shown in figure S6. The intramolecular hydrogen bonding was formed five membered cyclic ring motif and the structure was shown along a axis in figureS7 and the data were listed in table S4. The amide nitrogen and oxygen atom are formed intermolecular hydrogen bonding and the structural motif shown along a axis in figure S8. The one dimensional linear chain structure was generated. These building blocks are tailored alternatively and propagate as 3D dimensional supramolecular architecture along a axis as shown in figure S9.

The crystal structure **6b & 6d** obtained with two independent molecules per unit cell. The displacement ellipsoid plots of the structures were illustrated in figureS10 and their hydrogen bonding data were recorded in table S5 respectively. In the crystal structure the five member cyclic ring motif (Figure S11) were formed through intermolecular hydrogen bonding via O(4)-H(4)...N(3). The intermolecular hydrogen bonding was extended to form supramolecular zig-zag motif with graph set R22(16). The cumulative effects result in one dimensional supramolecular chain propagating along a axis as shown in figure S12. Stability of the crystal **6d** was enhanced by C−H…π interactions as it is demonstrated in figure S13.

2.3. DNA Binding Studies

2.3.1. DNA Absorbance Titration

The interaction between DNA and compounds were studied using UV visible spectroscopic methods. The intercalative mode of binding occurs via strong stacking interaction between the compound and DNA base pairs leading to hypochromism. The changes in the absorbance spectra of all the compounds (**4a - 4e & 6a- 6f**) upon addition of increasing concentration of DNA were monitored. The absorption of compounds **4a - 4e** and **6a - 6f** at various concentrations of DNA are displayed in Figure 3, S1 &S2 and the absorption parameters are shown in Table 4.

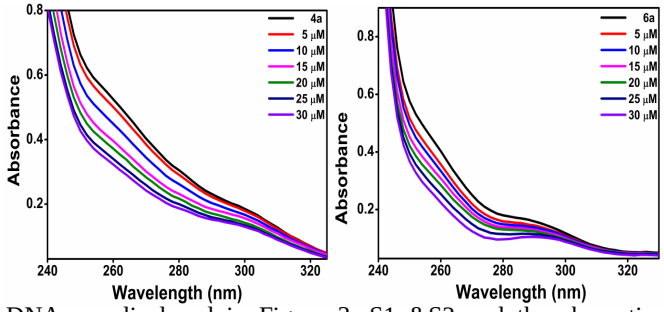

Figure 3. Adbsorbance titration spectra of compounds 4a & 6a.

Table 4. Binding constant, Stern Volmer constant, k_{app} and ΔG values of CT DNA-compound systems.

Compounds	K_b x 10^5 M^{-1}	-ΔG kJ mol^{-1}	K_{sv} x10^6 M^{-1}	K_{app} x10^6 M^{-1}
4a	10.54	34.94	3.79	2.49
4b	8.13	34.29	3.27	2.02
4c	9.77	34.75	3.73	2.40
4d	15.36	35.89	3.85	2.90
4e	20.50	37.01	3.95	2.95
6a	9.10	34.57	3.03	1.98
6b	6.05	33.54	2.80	1.89
6c	6.30	33.64	2.96	1.91
6d	7.75	34.17	3.02	1.92
6e	9.89	34.78	3.64	1.99
6f	10.91	35.03	3.81	1.20

The π- π* absorption band of the compounds **4a- 4e** and **6a - 6f** are shifted to ~2 nm bathochromic shift with hypochromism. The observed hypochromism suggests that the aromatic chromophore of the compounds (**4a - 4e** and **6a - 6f**) interact with CT DNA via intercalative mode of binding. [35]The binding constant values are calculated from Wolfee-Shimmer equation :[36]

$$[DNA]/(\varepsilon_a - \varepsilon_f) = [DNA]/(\varepsilon_a - \varepsilon_f) + 1/kb(\varepsilon_b - \varepsilon_f) \quad (1)$$

Where [DNA] is concentration of DNA, ε_a is the extinction coefficient of compound for a particular DNA concentration, ε_f is the extinction coefficient of free compound, and ε_b is the extinction coefficient of compound complex in fully bound form. The binding constant value is obtained from the ratio between the slope and intercept of plot $[DNA]/[\varepsilon_a-\varepsilon_f]$ versus [DNA] (Figure 4) .

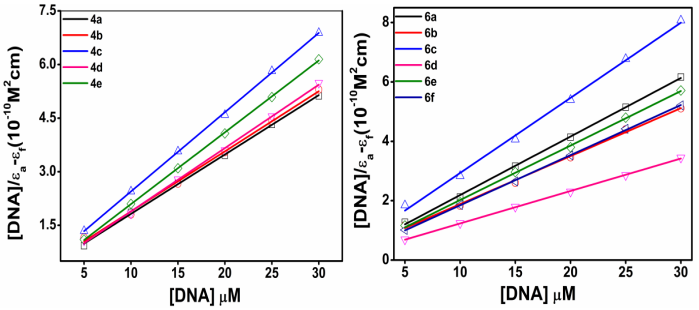

Figure 4. Wolfee-Shimmer plots of compounds 4a -4e and 6a- 6f.

All the compounds binding constant values are almost similar to EB binding constant (K_b= 1.23 x 10^5 M^{-1}) suggesting that all the compounds act as intercalators .[37] The strength of binding DNA with compounds was compared using K_b values of compounds. The high value of K_b indicates the high affinity towards DNA. The order of binding constant is 4e > 4d > 4a > 4c > 4b and 6f > 6e > 6a > 6d > 6c > 6b. This reveals that the electron releasing group present in the aromatic chromophore increases the strength of binding with DNA to a greater extent compared to the electron withdrawing groups. The free energy change (ΔG) for DNA- compounds was calculated using the following equation:

$$\Delta G = - 2.303\ RT \log K_b \quad (2)$$

-ΔG value of compound **4a - 4e** was found to be 37.01 kJ mol^{-1} - 34.28 kJ mol^{-1} and 35.02 kJ mol^{-1} – 33.54 kJ mol^{-1} for **6a - 6f**. This suggests that compounds - DNA intercalation mode of binding is a spontaneous process.

When comparing the **4a & 6a** compounds **4a** shows that high binding constant value. Due to the steric effect of morpholine ring intercalating efficiency was enhance for the **4a** compound.

2.3.2. Ethidium Bromide Displacement Assay

The effective technique to study the mode of binding of the compounds with DNA is fluorescence quenching assay using EB-bound DNA. EB is an intercalative indicator and it forms a soluble complex with DNA emitting an intense fluorescence. While adding a second intercalator to this solution, EB is replaced from EB-bound DNA thereby reducing the intensity of fluorescence of the system. [38] The fluorescence spectra of EB bound to DNA in the presence of compounds **4a - 4e** and **6a - 6f** are shown in Figure 5, S3 & S4.

The emission intensity was decreased while adding the compounds (**4a - 4e & 6a - 6f**) to EB- DNA system suggesting

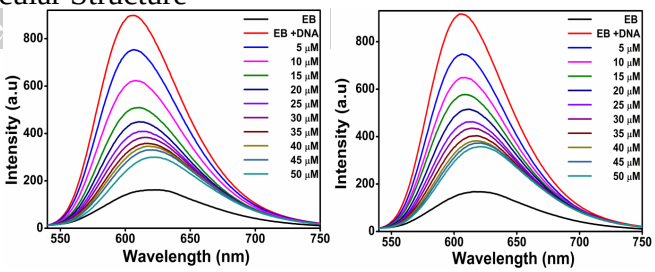

Figure 5. Emission spectra compounds 4a & 6a in EB-DNA system. (λex=520 nm, excitation slit=5nm, λemis slit= 5nm), and Fluorescence intensity at λemi 608nm for compounds (5μM))

that the EB was replaced by the compounds and EB is moving from hydrophobic environment to an aqueous environment.[39] At 598 nm the increase in concentration of compounds **4a - 4e** shows hypochromism up to 67%, 63%, 66%, 67% and 71% respectively with bathochromic shift 10-15nm. The compounds **6a – 6f** exhibit hypochromism up to 61%, 58%, 60%, 61%, 65% and 65% with a red shift of 10-15 nm. The fluorescence quenching was analysed by Stern Volmer equation :[40, 41]

$$F_0/F = 1 + K_{sv}[Q] \quad (3)$$

Where F_0 and F is the emission intensity in the absence and presence of the quencher, [Q] is the concentration of quencher, K_{sv} is the Stern Volmer quenching constant and K_{sv} is the slope that is obtained from a plot of F_0/F versus [Q] (Figure 6).

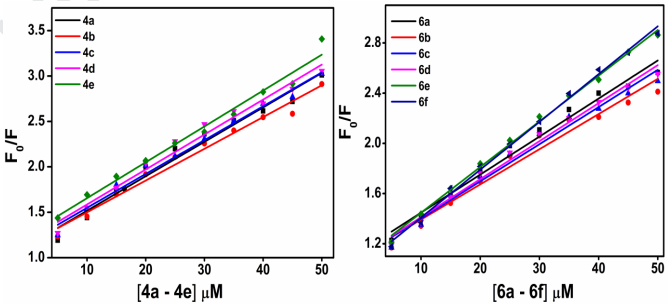

Figure 6. Stern Volmer plots of compounds 4a - 4e and 6a - 6f.

The Stern Volmer quenching constant (K_{sv}) values for **4a - 4e** were found to be 3.95×10^6 M^{-1} - 3.27×10^6 M^{-1} and for **6a - 6f** it is found to be 3.81 ×10^6 M^{-1} - 2.80 ×10^6 M^{-1} . A high value of K_{sv} indicates a greater binding ability towards DNA. Among these series 4 and 6, **4e** and **6f** have high binding ability with DNA. Furthermore, the apparent DNA binding constant (K_{app}) was calculated from the following equation :[42]

$$K_{EB}\,[EB] = K_{app}\,[Complex] \quad (4)$$

Where [complex] corresponds to 50% reduction of emission intensity of EB - bound DNA, and K_{EB} = 1.0 × 10^7 M^{-1}, [EB] = 5 μM. The K_{app} value of the compounds **4a – 4e** are 2.49 x10^6 M^{-1} , 2.02 x 10^6 M^{-1} , 2.40 x 10^6 M^{-1} , 2.90 x 10^6 M^{-1}, 2.95 x 10^6 M^{-1} respectively and for **6a - 6f** are 1.98 x 10^6 M^{-1}, 1.89 x 10^6 M^{-1}, 1.91 x 10^6 M^{-1}, 1.92 x 10^6 M^{-1}, 1.99 x 10^6 M^{-1}, 1.20 x10^6 M^{-1} respectively. The higher values for compounds **4e** and **6f** indicate that these compounds bind to DNA by intercalation.

2.4. Protein Binding Studies

2.4.1. UV Visible Spectral Studies

The UV visible spectroscopic studies are used to find the structural changes of proteins and to examine the protein – compound binding nature. The two types of quenching mechanism were involved, which are classified as dynamic and

static quenching mechanism.[43] The static quenching mechanism refers to compound – fluorophore complex formation. The dynamic quenching mechanism refers to fluorophore and compound interaction in the excited state. The absorbance spectra of BSA with the addition of compounds (**4a-4e & 6a – 6f**) are shown in Figure 7. The addition of compound to the BSA solution reveals hyperchromism without any shift in the wavelength. This suggests that in all the compounds, quenching is initiated by the static quenching mechanism.

2.4.2. Fluorescence Studies of BSA

The emission spectra of BSA with various concentrations of compounds **4a- 4e** and **6a - 6f** are shown in Figure 8, S4 & S5.

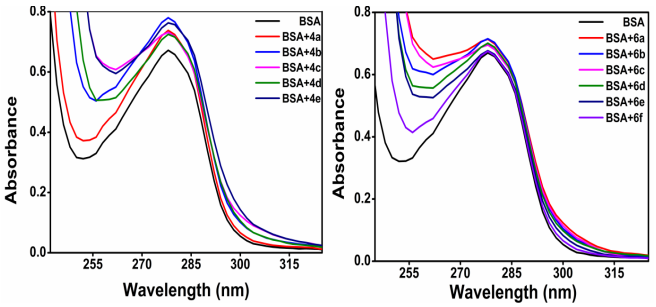

Figure 7. UV visible spectrums of BSA and compounds 4a-4e and 6a-6f with BSA.

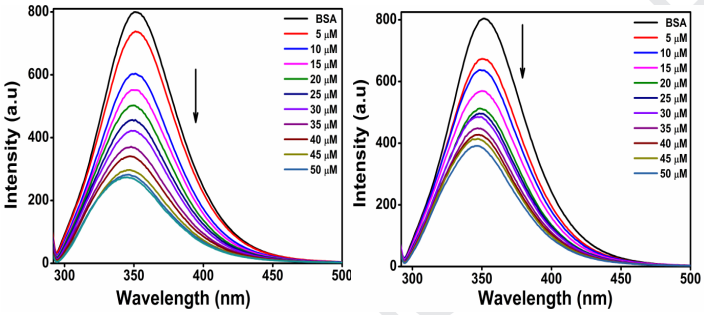

Figure 8. Emission spectra compounds 4a & 6a with BSA. (ex=280 nm, excitation slit=2.5nm, emission slit=2.5nm), and Fluorescence intensity at emission 350 nm for compounds (5μM))

While increasing the concentration of compounds, the intensity of emission spectrum of BSA gradually decreases from 73% - 55% for **4a - 4e** and from 66% - 45 % for **6a - 6f** with a hypsochromic shift of 2-3 nm. This suggests that all the compounds bind with BSA effectively and the fluorescence quenching is defined by the Stern–Volmer relation :[44, 45]

$$F_0/F = 1 + Kq\ \tau_0[Q] = 1 + K_{sv}[Q] \quad (5)$$

Where F_0 and F are the emission intensity in the absence and presence of the quencher, [Q] is the concentration of quencher, K_{sv} is the Stern–Volmer constant and K_{sv} is the slope that is obtained from a plot of F_0/F versus [Q] (Figure 9). K_q is bimolecular quenching constant and τ_0 is the average lifetime of BSA. Figure 9 shows the Stern Volmer plots of **4a - 4e** and **6a - 6f** and K_q and K_{sv} value are displayed in Table 5.

The obtained Kq values of compounds 4a - 4e (5.51 x 1012 M-1 s-1 - 2.27 x 1012 M-1 s-1) and 6a - 6f (3.83 x 1012 M-1 s-1 - 1.44 x 1012 M-1 s-1) are two-fold higher (2 x 1010 M-1 s-1) than the maximum value possible for diffusion controlled quenching.[46] These K_q values suggest that all the compounds follow the static quenching mechanism. The K_{sv} values show that **4e** (5.51x 10^5 M^{-1}) and **6f** (3.83x 10^5 M^{-1}) have high binding affinity towards BSA.

Table 5. BSA binding parameters of the compounds 4a - 4e & 6a - 6f.

Compound	K_{sv} x10^5 M^{-1}	K_q x10^{12} $M^{-1}s^{-1}$	K x10^6 M^{-1}	n	ΔG kJ mol^{-1}
4a	3.83	3.83	3.82	0.83	-38.19
4b	2.27	2.27	3.35	0.77	-37.86
4c	2.58	2.58	3.74	0.84	-38.13
4d	4.34	4.34	4.23	0.90	-38.44
4e	5.51	5.51	4.55	0.96	-38.63
6a	2.61	2.61	3.29	0.76	-37.80
6b	1.44	1.44	2.68	0.64	-37.29
6c	1.89	1.88	2.96	0.64	-37.55
6d	2.51	2.51	3.15	0.69	-37.70
6e	2.71	2.71	3.64	0.82	-38.07
6f	3.83	3.83	4.14	0.90	-38.39

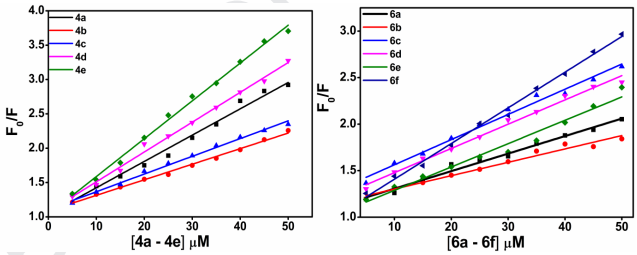

Figure 9. Stern Volmer Plot of 4a- 4e and 6a- 6f.

2.4.3. Binding Constant and Number of Binding Sites

Generally small molecules bind with sets of equivalent sites on macromolecules, with the equilibrium between the bound and free molecules analysed according to the Scatchard equation :[47]

$$\log[(F_0\text{-}F)/F] = \log K + n \log[Q] \quad (6)$$

Where K is the binding constant and n is the number of binding sites respectively. The value of K and n values are determined from the slope and intercept of log $[(F_0\text{-}F)/F]$ versus log[Q] . The Scatchard plots of compounds **4a - 4e** and **6a - 6f** are shown in Figure 10 and the resultant binding constant K and number of binding sites is shown in Table 5.

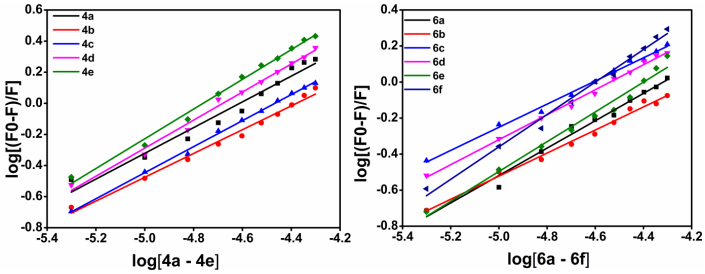

Figure 10. Scatchard plots of compounds 4a- 4e and 6a- 6f.

The order of binding constant values of **4a - 4e** (4.55 x 10^6 M^{-1} - 3.82 x 10^6 M^{-1}) and **6a - 6f** (4.14 x 10^6 M^{-1}- 2.68 x 10^6 M^{-1}) are: 4e > 4d > 4a > 4c > 4b and 6f > 6e > 6a > 6d > 6c > 6b. The values of n for all the compounds around 1 indicate that all the compounds have a single binding site in BSA .[48]

The free energy changes were analysed when the compounds bind with BSA and are shown in Table 5. The ΔG values of **4a -**

4e are from -38.63 kJ mol^{-1} to -38.19 kJ mol^{-1}. The ΔG values of 6a – 6f are from -38.39 kJ mol^{-1} to -37.29 kJ mol^{-1}. Negative values of ΔG suggest that binding process of all the compounds are spontaneous and favourable process .[49]

2.4.4. BSA Conformational Analysis

Synchronous emission spectroscopy gives information on the molecular environment in the vicinity of tyrosine and tryptophan residues present in the BSA. The fluorophore characteristic Δλ value is 15 nm for the tyrosine residues and 60 nm for tryptophan residues.[50] The Synchronous emission spectra of BSA with various concentrations of compounds are shown in Figure 11, 12 & S7- S10. In the synchronous fluorescence spectra at Δλ = 15 nm, in the BSA solution, increased addition of compounds **4a - 4e** and **6a - 6f** exhibit the hypochromism of 61% - 45% and 48% -31% respectively with 2-3 nm bathochromic shift. In the Δλ = 60 nm spectra, decreased fluorescence intensity is observed for **4a – 4e** from 70% to 59% .and it is from 61% to 51% for **6a – 6f** without any significant shift. The intensity of the fluorescence is quenched for both the tyrosine and tryptophan residues.

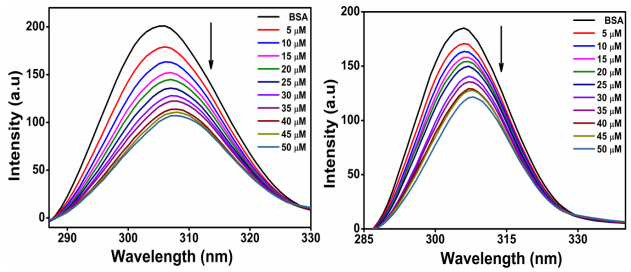

Figure 11. Synchronous Fluorescence spectra of BSA - compounds 4a & 6a with Δλ= 15 nm.

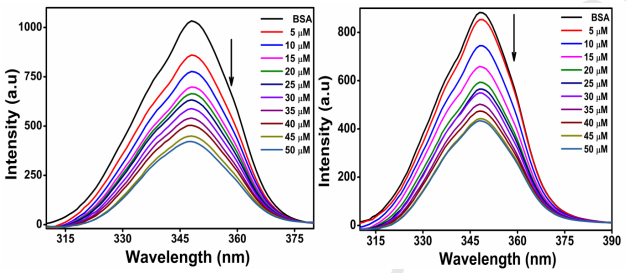

Figure 12. Synchronous Fluorescence spectra of BSA - compounds 4a & 6a with Δλ= 60 nm.

These results indicate that conformation changes, increase in hydrophobicity of the environment and decrease in the polarity of the fluorophore have occurred.[51, 52]

3. Conclusion

In conclusion, the simple and one pot multi-component procedure has been described for the synthesis of amino-aryl methylated paracetamol derivatives. Variation in secondary amine afforded all the products in moderate to good yield. The mechanism of the amino aryl methylation of paracetamol has been explained. The compounds are interacting with CT DNA via intercalation mode of binding and confirmed through UV visible and EB displacement assay studies. The binding constant values were determined. The increasing order of DNA binding ability is 4b < 4c < 4 a < 4d < 4e; 6b < 6c < 6 d < 6a < 6e < 6f. Further, the compounds bind with BSA through static mode of binding. The binding constant values show that BSA binding ability with compounds is in the order 4b < 4c < 4 a < 4d < 4e; 6b < 6c < 6 d < 6a < 6e < 6f. The confirmation analysis of BSA protein binding results revealed that the compounds affect the microenvironment around the tryptophan and tyrosine residues. Negative values of ΔG indicate that CT DNA and BSA binding with all the compounds are spontaneous and favorable process.

4. Experimental Section

4.1. General Procedure for the Synthesis of 4a - 4e and 6a - 6f

The optimization of the reaction and results are presented in Table 1-3. 5 mmol of paracetamol **3** was dissolved in isopropyl alcohol solution. To this solution 5 mmol amine (Piperidine **2** /morpholine **5**) was added followed by drop wise addition of 5 mmol benzaldehyde **1**. The resulting solution was refluxed for 24 hours. The reaction completion was monitored by TLC. The solvent was removed under reduced pressure and washed with distilled water and acetone.

4.2. DNA Binding Studies

UV visible absorption titration was carried out for all the compounds at a concentration of 10μM with incremental addition of CT DNA (5-30 μM in sodium phosphate buffer solution, pH ~7.2). The purity of the CT DNA was confirmed by absorption ratio of CT DNA at 260 and 280 nm which was found to be 1.9:1 indicating it is sufficiently free from protein. The concentration of CT DNA was calculated from the known molar extinction coefficient (ε = 6600 M^{-1} cm^{-1}) and absorbance intensity at 260 nm. Ethidium bromide (EtBr) displacement studies were carried out by monitoring the changes in the fluorescence intensity at excitation and emission wavelengths of 525 and 602 nm upon increasing the concentration of compounds (**4a - 4e & 6a - 6f**) from 5 -50 μM in an aqueous solution of the EtBr-DNA.

4.3. Protein Binding Studies

In the protein binding studies, the excitation wavelength of BSA at 280 was fixed and the emission changes were monitored at ~348 nm using BSA (0.5 μM) solution prepared in phosphate buffer (pH ~7.5). 2.5 mL of BSA solution was titrated with various concentrations (5 - 50μM) of compounds **4a - 4e** and **6a - 6f**. Synchronous fluorescence spectral studies with two different Δλ values of 15 and 60 nm were carried out with similar concentrations.

4a: White, Solid, m.p. 210 °C, $[\alpha]_D^{20}$ = 0.40° at C=0.5 in MeOH, FTIR (KBr) ν_{max} (cm^{-1}): (N-H) 3270, 1555, (O-H) 3149, (Ar C-H) 3086, (Ali C-H) 2936, 2816, 1443, 1373, (C=O) 1657, (C-O) 1251, (C-N-C) 1149, 1092, 1065, 1036,1018; ^{1}H NMR (400 MHz, DMSO-d_6 : D_2O (~ 20:1 v/v)) δ/ ppm: 11.07 (s, 1H), 9.63 (s, 1H), 7.40 (s, 1H), 7.38 (s, 1H), 7.23-7.33 (m, 5H), 6.65 (d, J = 8.40 Hz, 1H), 4.57 (s, 1H), 2.30-2.51 (t, 4H), 1.93 (s, 3H), 1.11-1.53 (m, 6H) ^{13} C NMR (400 MHz, DMSO-d_6 : D_2O (~ 20:1 v/v))δ/ppm.: 167.93 (C=O), 152.12 (C-O) , 128.59 (N-C), 141.44, 131.57,129.00, 128.59, 127.74, 127.17, 120.21, 119.67, 116.23 (Ar-C), 72.60 (Methine), 52.53, 26.11 (Pi), 24.18 (Methyl); HRMS (m/z): [M-H] Calc: 323.18 found: 323.22.

4b: White, Solid, m.p. 185 °C, $[\alpha]_D^{20}$ = 1.00° at C=0.5 in MeOH, FTIR (KBr) ν_{max} (cm^{-1}): (N-H) 3227, 1559, (O-H) 3139, (Ar C-H) 3067, (Ali C-H) 2927, 2816, 1456, 1386, (C=O) 1659, (C-O) 1258, (C-N-C) 1152, 1108, 1091, 1058, 1036, 1008; ^{1}H NMR (300 MHz, DMSO-d_6 : D_2O (~ 20:1 v/v))δ/ ppm : 10.70 (s, 1H), 9.61 (s, 1H), 7.39 (d, J = 1.50 Hz, 1H), 7.31 (d, J = 7.80 Hz, 2H), 7.24 (d, J = 8.70 Hz, 1H), 6.64 (d, J = 8.70 Hz, 2H), 7.09 (d, J = 7.80 Hz, 2H), 4.49 (s, 1H), 2.45 (m,4H), 2.24 (s, 3H), 1.73-1.95 (m, 6H); ^{13} C NMR (300 MHz, DMSO-d_6 : D_2O (~ 20:1 v/v))δ/ppm: 167.47 (C=O), 151.02 (C-O) , 136.10 (C-Cl), 131.03 (N-C), 140.10, 128.86, 128.26, 127.32, 119.31, 119.09, 115.51 (Ar-C), 70.54 (Methine), 52.60, 23.64, 20.56 (Pi), 23.09 (Methyl); HRMS (m/z): [M+H] Calc: 359.14 found: 359.16.

4c: White, Solid, m.p. 192 °C, $[\alpha]_D^{20}$ = 0.00° at C=0.5 in MeOH, FTIR (KBr) ν_{max} (cm^{-1}): (N-H) 3250, 1548, (O-H) 3144, (Ar C-H) 3078, (Ali C-H) 2916, 2849, 1447, 1364, (C=O) 1659, (C-O) 1242, (C-N-C) 1158, 1108, 1069, 1053, 1042,1017; ^{1}H NMR (500 MHz, DMSO-d_6 : D_2O (~ 20:1 v/v)) δ/ppm: 10.77 (s, 1H), 9.63 (s, 1H), 7.52 (s, 1H), 7.51 (s, 1H), 7.34 (d, J = 10.00 Hz, 2H), 7.29 (d, J = 5.00 Hz, 2H), 6.66 (d, J = 10.00 Hz, 1H), 4.63 (s, 1H), 2.39 (m, 4H), 1.94 (s, 3H), 1.40-1.52 (m, 6H); ^{13} C NMR (500 MHz, DMSO-d_6 : D_2O (~ 20:1 v/v)) δ/ppm: 167.94 (C=O), 151.97 (C-O), 120.70 (C-Br), 131.69 (N-C),140.99, 131.85, 130.78, 126.33, 120.2, 119.78, 116.23 (Ar-C) 79.65 (Methine), 52.46, 26.11, 24.31 (Pi), 24.19, (Methyl) ; HRMS (m/z) : [M+H] Calc: 403.09, found: 403.09.

4d: White, Solid, m.p. 211 °C, $[\alpha]_D^{20}$ = -0.60° at C=0.5 in MeOH, FTIR (KBr) ν_{max} (cm^{-1}): (N-H) 3261, 1564, (O-H) 3150, (Ar C-H) 3089, (Ali C-H) 2922, 2844, 1447, 1392, (C=O) 1648, (C-O) 1242, (C-N-C) 1152, 1108, 1091, 1053, 1030, 1019; 1H NMR (500 MHz, DMSO-d_6 : D_2O (~ 20:1 v/v)) δ/ppm: 11.24 (s, 1H), 9.60 (s, 1H), 7.28 (s, 1H), 7.26 (d, J = 5.00 Hz, 2H), 7.24 (d, J = Hz, 1H), 7.13 (d, J = 5.00 Hz, 2H), 6.65 (d, J = 10.00 Hz, 1H), 4.55 (s, 1H), 2.40 (m, 4H), 2.26 (s, 3H), 1.93 (s, 3H), 1.40-1.50 (m, 6H) ; ^{13} C NMR (500 MHz, DMSO-d_6 : D_2O (~ 20:1 v/v)) δ/ppm: 167.89 (C=O), 152.30 (C-O) ,136.95 (C-Me), 129.54 (N-C), 128.62, 120.32, 119.67, 116.22 (Ar-C) , 72.66 (Methine), 52.39, 26.12, 24.27 (Pi), 24.17, 21.10(Methyl) ; HRMS (m/z): [M+H] Calc: 339.20, found: 339.30.

4e: White, Solid, m.p. 198 °C, $[\alpha]_D^{20}$ = -1.60° at C=0.5 in MeOH, FTIR (KBr) ν_{max} (cm^{-1}): (N-H) 3278, 1553, (O-H) 3144, (Ar C-H) 3083, (Ali C-H) 2938, 2861, 1436, 1375, (C=O) 1648, (C-O) 1231, (C-N-C) 1180, 1152, 1064, 1091; ^{1}H NMR (500 MHz, DMSO-d_6 : D_2O (~ 20:1 v/v)) δ/ppm: 11.38 (s, 1H), 9.59 (s, 1H), 7.31 (s, 1H), 7.28 (d, J = 10.00 Hz, 2H), 7.24 (d, J = 10.00 Hz, 1H), 7.69 (d, J = 5.00 Hz, 2H), 6.67 (d, J = 5.00 Hz, 1H), 4.53 (s, 1H), 2.40 (m, 4H), 3.72 (s, 3H), 1.96(s, 3H) ,1.39-1.52 (m, 6H); ^{13} C NMR (500 MHz, DMSO-d_6 : D_2O (~ 20:1 v/v)) δ/ppm: 167.90 (C=O), 158.96, 152.42 (C-O) , 131.49 (N-C), 132.81, 129.91, 127.13, 120.43, 119.72, 116.27, 114.34 (Ar-C), 72.68 (Methine), 55.47 (Methoxy), 52.32, 26.14, 24.26 (Pi), 24.15(Methyl); HRMS (m/z): [M-H] Calc: 353.19 found: 353.19.

6a: White, Solid, m.p. 218 °C, $[\alpha]_D^{20}$ = 0.40° at C=0.5 in MeOH, FTIR (KBr) ν_{max} (cm^{-1}): (N-H) 3299, 1556, (O-H) 3199, (Ar C-H) 3073, (Ali C-H) 2973, 2947, 1443, 1385, (C=O) 1650, (C-O) 1252, (C-O-C) 1117, (C-N-C) 1157, 1124, 1023, 1006; ^{1}H NMR (400 MHz, DMSO-d_6 : D_2O (~ 20:1 v/v)) δ/ppm: 10.12 (s, 1H), 9.70 (s, 1H), 7.48 (s, 1H), 7.29-7.43 (m, 5H), 7.21 (t, J = 7.60 Hz, 1H), 6.69 (d, J = 8.80 Hz, 1H), 4.61 (s, 1H), 3.61 (s, 4H), 2.32 (t, J = 10.00 Hz, 4H) 1.97 (s, 3H); ^{13} C NMR (400 MHz, DMSO-d_6 : D_2O (~ 20:1 v/v), δ/ppm: 168.04 (C=O), 151.43 (C-O), 131.80 (N-C), 141.71, 128.94, 128.50, 127.56, 127.35, 119.90, 119.65, 116.05 (Ar-C) , 70.40 (Methine), 66.70 (O-CH_2), 52.51 (N-CH_2), 24.19 (Methyl); HRMS (m/z): [M-H] Calc: 325.16, found: 325.17.

6b: White, Solid, m.p. 213 °C, $[\alpha]_D^{20}$ = -1.40° at C=0.5 in MeOH, FTIR (KBr) ν_{max} (cm^{-1}): (N-H) 3283, 1559, (O-H) 3150, (Ar C-H) 3089, (Ali C-H) 2955, 2810, 1456, 1386, (C=O) 1653, (C-O) 1244, (C-O-C) 1118, (C-N-C) 1152, 1108, 1091, 1058, 1036, 1008; ^{1}H NMR (400 MHz, DMSO-d_6 : D_2O (~ 20:1 v/v)) δ/ppm: 9.90 (s, 1H), 9.58 (s, 1H), 7.38 (s, 1H), 7.35 (t, J = 10.00 Hz, 2H), 7.21 (d, J = 8.40 Hz, 1H), 7.06 (t, J = 8.40 Hz, 2H), 6.60 (d, J = 8.80 Hz, 1H), 4.59 (s, 1H), 3.53 (s, 4H), 2.25 (t, J = 6.40 Hz, 4H), 1.89 (s, 3H); ^{13} C NMR (400 MHz, DMSO-d_6 : D_2O (~ 20:1 v/v), δ/ppm: 167.97 (C=O), 151.34 (C-O), 162.82, 160.41(C-F), 131.88 (N-C), 137.95, 130.40, 130.32, 127. 28, 119.74, 119.70, 116.08, 116.56, 116.55 (Ar-C) , 70.40 (Methine), 66.70 (O-CH_2), 52.51 (N-CH_2), 24.19(Methyl); HRMS (m/z): [M-H] Calc: 343.15, found: 343.15.

6c: White, Solid, m.p. 202 °C, $[\alpha]_D^{20}$ = 1.60° at C=0.5 in MeOH, FTIR (KBr) ν_{max} (cm^{-1}): (N-H) 3298, 1560, (O-H) 3212, (Ar C-H) 3101, (Ali C-H) 2960, 2838, 1493, 1382, (C=O) 1660, (C-O) 1252, (C-O-C) 1111, (C-N-C) 1156, 1111, 1016; ^{1}H NMR (400 MHz, DMSO-d_6 : D_2O (~ 20:1 v/v)) δ/ppm: 9.81 (s, 1H), 9.59 (s, 1H), 7.39 (s, 1H), 7.31 (dd, J = 8.40, 10.80 Hz, 4H), 7.22 (d, J = 8.80 Hz, 1H), 6.60 (d, J = 8.80 Hz, 1H), 4.57 (s, 1H), 3.53 (s, 4H), 2.24 (t, J=6.80 Hz, 4H), 1.89 (s, 3H); ^{13} C NMR (400 MHz, DMSO-d_6 : D_2O (~ 20:1 v/v)) δ/ppm: 167.97 (C=O), 151.31 (C-O), 131.97 (C-Cl), 131.91 (N-C), 140.92, 130.28, 127.05, 119.73, 119.66, 116.04 (Ar-C), 68.80 (Methine),66.71 (O-CH_2), 52.44 (N-CH_2), 24.21 (Methyl); HRMS (m/z): [M+H] Calc: 361.12, found: 361.00.

6d: White, Solid, m.p. 218 °C, $[\alpha]_D^{20}$ = 1.60° at C=0.5 in MeOH, FTIR (KBr) ν_{max} (cm^{-1}): (N-H) 3277, 1548, (O-H) 3200, (Ar C-H) 3090, (Ali C-H) 2970, 2851, 1441, 1382, (C=O) 1655, (C-O) 1247, (C-O-C) 1117, (C-N-C) 1134, 1099, 1066, 1023; ^{1}H NMR (500 MHz, DMSO-d_6 : D_2O (~ 20:1 v/v)) δ/ppm: 9.87 (s, 1H), 9.64 (s, 1H), 7.50 (d, J = 10.00 Hz, 2H), 7.45 (s, 1H), 7.35 (d, J = 10.00 Hz, 2H), 7.29 (d, J = 10.00 Hz, 1H), 6.68 (d, J = 10.00 Hz, 1H), 4.63 (s, 1H), 3.60 (s, 4H), 2.30 (t, J = 10.00 Hz, 4H), 1.96 (s, 3H); ^{13} C NMR (500 MHz, DMSO-d_6 : D_2O (~ 20:1 v/v)) δ/ppm: 167.97 (C=O), 151.53 (C-O), 120.49 (C-Br), 131.80 (N-C), 141.35, 131.92, 130.66, 126.98, 119.78, 119.73, 160.06 (Ar-C) , 68.89 (Methine), 66.72 (O-CH_2), 52.43 (N-CH_2), 24.19 (Methyl); HRMS (m/z): [M-H] Calc: 403.07 found: 403.04.

6e: White, Solid, m.p. 223 °C, $[\alpha]_D^{20}$ = -0.80° at C=0.5 in MeOH, FTIR (KBr) ν_{max} (cm^{-1}) : N-H 3311, 1553, (O-H) 3100, (Ar C-H) 3032, (Ali C-H) 2977, 2855, 1447, 1386, (C=O) 1653, (C-O) 1242, (C-O-C) 1113, (C-N-C) 1108, 1075, 1030, 1019; ^{1}H NMR (500 MHz, DMSO-d_6 : D_2O (~ 20:1 v/v)) δ/ppm: 10.18 (s, 1H), 9.65 (s, 1H), 7.43 (s, 1H), 7.31 (d, J = 5.00 Hz, 2H), 7.29 (s, 1H), 7.11 (d, J = 10.00 Hz, 2H), 6.68 (d, J = 10.00 Hz, 1H), 4.57 (s, 1H), 3.61 (s, 4H), 2.32 (t, J = 10.00 Hz, 4H), 2.24 (s, 3H) ^{13} C NMR (500 MHz, DMSO-d_6 : D2O (~ 20:1 v/v)) δ/ppm: 167.95 (C=O), 151.49 (C-O), 136.74 (C-Me), 131.80 (N-C), 138.53, 129.50, 128.48, 127.36, 119.99, 119.62, 116.06 (Ar-C), 70.51 (Methine) ,66.72 (O-CH_2), 52.45 (N-CH_2), 24.20, 21.08 (Methyl); HRMS (m/z): [M-H] Calc: 339.18 found: 339.30.

6f: White, Solid, m.p. 229 °C, $[\alpha]_D^{20}$ = -0.20° at C=0.5 in MeOH, FTIR (KBr) ν_{max} (cm^{-1}): (N-H) 3278, 1553, (O-H) 3144, (Ar C-H) 3083, (Ali C-H) 2938, 2861, 1436, 1375, (C=O) 1648, (C-O) 1242, (C-O-C) 1108, (C-N-C) 1180, 1152, 1091, 1064; ^{1}H NMR (500 MHz, DMSO-d_6 : D_2O (~ 20:1 v/v)) δ/ppm: 10.22 (s, 1H), 9.64 (s, 1H), 7.42 (s, 1H), 7.31 (d, J = 10.00 Hz, 2H), 7.28 (d, J = 5.00 Hz, 1H), 6.87 (d, J = 10.00 Hz, 2H), 6.67 (d, J = 5.00 Hz, 1H), 4.54 (s, 1H), 3.71 (s, 3H), 3.60 (s, 4H), 2.31 (t, J = 10.00 Hz, 4H); ^{13} C NMR (500 MHz, DMSO-d_6 : D2O (~ 20:1 v/v)) δ/ppm: 167.95 (C=O), 151.47, (C-O), 158.80 (C-OMe), 131.79 (N-C), 133.33,129.71, 127.49, 119.92, 119.55, 116.08, 114.33 (Ar-C), 70.28 (Methine), 66.72 (O-CH_2), 52.41(N-CH_2), 55.48 (Methoxy), 24.20 (Methyl); HRMS (m/z): [M-H] Calc: 355.17 found: 355.16.

Crystal structure data for 4a (CCDC 1403704),C_{20} H_{24} N_2 O_2 M_r = 324.41, ortho rhombic, P2na2$_1$, a = 8.7696(4) A° , b = 19.6874(11) A° , C = 10.4825(6) A° , α = 90°, β = 90° , ϒ = 90° , V ($Å^3$)= 1809.81(17), T= 296 K, Z = 4, D^x = 1.191 (mg/m^3), μ (mm^{-1}) = 0.077, F(000) = 696.

Crystal structure data for 4b (CCDC 1556655) , C_{20} H_{23} Cl N_2 O_2: M_r = 358.85, Monoclinic, $P2_1/c$, a =13.5097(6) A°, b =15.5363(7) A°, C =9.1134(4) A° , α = 90°, β =104.290(9)°, ϒ = 90° , V (Å^3) = 1853.63(16), T = 293 K, Z = 4, D_x = 1.286 (mg/m^3), μ (mm^{-1}) = 0.222, F(000) = 760.

Crystal structure data for 4c (CCDC 1556656) , C_{20} H_{23} Br N_2 O_2: M_r= 403.31, Monoclinic, $P2_1/c$, a = 13.857(2) A°, b = 9.6010(12)A°, C =15.525(2) A°, α = 90°, β = 113.235(6)° , ϒ = 90°, V (Å^3)= 1898.0(5), T= 296 K, Z = 4, D_x = 1.411 (mg/m^3), μ (mm^{-1}) = 2.181, F(000) = 832.

Crystal structure data for 4d (CCDC 1556657) ,C_{21} H_{26} N_2 O_2 : M_r= 338.44, monoclinic, $P2_1/c$, a =13.777(3)A°, b =9.635(2) A°, C =15.495(3) A° , α = 90°, β = 113.939(5)° , ϒ = 90° , V (Å^3)= 1880.00(7), T= 293 K, Z = 4, D_x = 1.196 (mg/m^3), μ (mm^{-1}) = 0.077, F(000) = 728.

Crystal structure data for 4e (CCDC 1556658), C_{21} H_{26} N_2 O_3 : M_r= 354.44, monoclinic, $P2_1/c$, a =13.9410(6) A°, b =9.7501(4) A°, C =14.9428(6) A°, α =90°, β =115.5490(10)°, ϒ= 90° , V (Å^3)= 1889.15(14), T= 296 K, Z = 4, D_x = 1.246 (mg/m^3), μ (mm^{-1}) = 0.084, F(000) = 760.

Crystal structure data for 6a (CCDC 1402257) , C_{19} H_{22} N_2 O_3 : M_r = 326.38, monoclinic, $P12_1/c1$, a =10.7158(3) A°, b = 17.0330(5) A°, C = 9.4162(3) A° , α = 90°, β = 91.7240(10)°, ϒ= 90°,V (Å^3) = 1717.89(9), T = 296 K, Z = 4, D_x = 1.262 (mg/m^3), μ (mm^{-1}) = 0.086, F(000) = 696.

Crystal structure data for 6b (CCDC 1556659), C_{19} H_{21} F N_2 O_3 : M_r = 344.38, monoclinic, $P2_1/n$, a = 9.2672(5) A°, b =10.0443(6) A°, C=37.974(2) A° , α = 90°, β = 90.821(4)° , ϒ = 90° , V (Å^3)= 3534.40(4), T= 296 K, Z = 8, D_x = 1.294 (mg/m^3), μ (mm^{-1}) = 0.095, F(000) = 1456.

Crystal structure data for 6d (CCDC 1435610),C_{19} H_{21} Br N_2 O_3 : M_r = 405.29, monoclinic, $P2_1$, a = 9.1943(9) A°, b =10.2358(10) A°, c =19.7750(2) A°, α = 90°, β = 90.487(3)°, ϒ = 90°, V (Å^3)= 1861.00(3), T= 293 K, Z = 4, D_x = 1.447 (mg/m^3), μ (mm^{-1}) = 2.229, F(000) = 832.

Crystal structure data for 6e (CCDC 1570809),C_{20} H_{24} N_2 O_3 : M_r = 340.41, monoclinic, $P2_1/c$, a = 11.4005(11) A°, b = 17.3367(16) A°, c = 9.3671(8) A°, α = 90°, β = 90.384(4)°, ϒ = 90°, V (Å^3) = 1851.3(3), T = 296 K, Z = 4, D_x = 1.221 (mg/m^3), μ (mm^{-1}) = 0.082, F(000) = 728.

References and notes

[1] C. de Graaff, E. Ruijter, R.V. Orru, Recent developments in asymmetric multicomponent reactions, Chem. Soc. Rev. 41(10) (2012) 3969-4009.

[2] A. Dömling, Recent developments in isocyanide based multicomponent reactions in applied chemistry, Chem. Rev. 106(1) (2006) 17-89.

[3] E. Wei, B. Liu, S. Lin, F. Liang, Multicomponent reaction of chalcones, malononitrile and DMF leading to γ-ketoamides, Org. Biomol. Chem. 12(33) (2014) 6389-6392.

[4] N. Isambert, M.d.M.S. Duque, J.-C. Plaquevent, Y. Genisson, J. Rodriguez, T. Constantieux, Multicomponent reactions and ionic liquids: a perfect synergy for eco-compatible heterocyclic synthesis, Chem. Soc. Rev. 40(3) (2011) 1347-1357.

[5] X. Xin, Y. Wang, S. Kumar, X. Liu, Y. Lin, D. Dong, Efficient one-pot synthesis of substituted pyridines through multicomponent reaction, Org. Biomol. Chem. 8(13) (2010) 3078-3082.

[6] H.-J. Wang, L.-P. Mo, Z.-H. Zhang, Cerium ammonium nitrate-catalyzed multicomponent reaction for efficient synthesis of functionalized tetrahydropyridines, ACS Comb. Sci. 13(2) (2010) 181-185.

[7] M.S. Singh, S. Chowdhury, Recent developments in solvent-free multicomponent reactions: a perfect synergy for eco-compatible organic synthesis, RSC Adv. 2(11) (2012) 4547-4592.

[8] D. Naskar, A. Roy, W.L. Seibel, D.E. Portlock, Novel Petasis boronic acid–Mannich reactions with tertiary aromatic amines, Tetrahedron Lett. 44(31) (2003) 5819-5821.

[9] J. Zhen, Y. Dai, T. Villani, D. Giurleo, J.E. Simon, Q. Wu, Synthesis of novel flavonoid alkaloids as α-glucosidase inhibitors, Bioorg. Med. Chem. (2017).

[10] L. El Kaim, L. Grimaud, J. Oble, New ortho-quinone methide formation: application to three-component coupling of isocyanides, aldehydes and phenols, Org. Biomol. Chem. 4(18) (2006) 3410-3413.

[11] G. Song, M. Jin, Z. Li, P. Ouyang, Asymmetric synthesis of α, β-diamino acid derivates via Mannich-type reactions of a chiral Ni (II) complex of glycine with N-tosyl imines, Org. Biomol. Chem. 9(20) (2011) 7144-7150.

[12] R.D. Wavhale, E.A. Martis, P.K. Ambre, B. Wan, S.G. Franzblau, K.R. Iyer, K. Raikuvar, K. Macegoniuk, Ł. Berlicki, S.R. Nandan, Discovery of new leads against Mycobacterium tuberculosis using scaffold hopping and shape based similarity, Bioorg. Med. Chem. 25(17) (2017) 4835-4844.

[13] Y.-Q. Wang, X.-Y. Cui, Y.-Y. Ren, Y. Zhang, A highly enantioselective and regioselective organocatalytic direct Mannich reaction of methyl alkyl ketones with cyclic imines benzo [e][1, 2, 3] oxathiazine 2, 2-dioxides, Org. Biomol. Chem. 12(45) (2014) 9101-9104.

[14] S.M. Kim, J.W. Yang, Organocatalytic asymmetric synthesis of β 3-amino acid derivatives, Org. Biomol. Chem. 11(29) (2013) 4737-4749.

[15] X. Li, C.-h. Yeung, A.S. Chan, T.-K. Yang, New 1, 3-amino alcohols derived from ketopinic acid and their application in catalytic enantioselective reduction of prochiral ketones, Tetrahedron: Asymmetry 10(4) (1999) 759-763.

[16] A. Bertolini, A. Ferrari, A. Ottani, S. Guerzoni, R. Tacchi, S. Leone, Paracetamol: new vistas of an old drug, CNS Drug Rev. 12(3□4) (2006) 250-275.

[17] Y.-J.J. Wu, A.J. Neuwelt, L.L. Muldoon, E.A. Neuwelt, Acetaminophen enhances cisplatin-and paclitaxel-mediated cytotoxicity to SKOV3 human ovarian carcinoma, Anticancer Res. 33(6) (2013) 2391-2400.

[18] G.F. Merrill, J.H. Merrill, R. Golfetti, K.M. Jaques, N.S. Hadzimichalis, S.S. Baliga, T.H. Rork, Antiarrhythmic properties of acetaminophen in the dog, Exp. Biol. Med. 232(9) (2007) 1245-1252.

[19] P.M. O'Neill, A. Mukhtar, P.A. Stocks, L.E. Randle, S. Hindley, S.A. Ward, R.C. Storr, J.F. Bickley, I.A. O'Neil, J.L. Maggs, Isoquine and related amodiaquine analogues: a new generation of improved 4-aminoquinoline antimalarials, J. Med. Chem. 46(23) (2003) 4933-4945.

[20] D. Sriram, R.V. Devakaram, M. Dinakaran, P. Yogeeswari, Aromatic amino analogues of artemisinin: synthesis and in vivo antimalarial activity, Med. Chem. Res. 19(6) (2010) 524-532.

[21] A. Chipeleme, J. Gut, P.J. Rosenthal, K. Chibale, Synthesis and biological evaluation of phenolic Mannich bases of benzaldehyde and (thio) semicarbazone derivatives against the cysteine protease falcipain-2 and a chloroquine resistant strain of

Plasmodium falciparum, Bioorg. Med. Chem. 15(1) (2007) 273-282.
[22] M.-J.R. Queiroz, E.M. Castanheira, M.S.D. Carvalho, A.S. Abreu, P.M. Ferreira, H. Karadeniz, A. Erdem, New tetracyclic heteroaromatic compounds based on dehydroamino acids: photophysical and electrochemical studies of interaction with DNA, Tetrahedron 64(2) (2008) 382-391.
[23] A. Kamal, N. Shankaraiah, C.R. Reddy, S. Prabhakar, N. Markandeya, H.K. Srivastava, G.N. Sastry, Synthesis of bis-1, 2, 3-triazolo-bridged unsymmetrical pyrrolobenzodiazepine trimers via 'click'chemistry and their DNA-binding studies, Tetrahedron 66(29) (2010) 5498-5506.
[24] A. Kaźmierska, M. Gryl, K. Stadnicka, L. Sieroń, A. Eilmes, J. Nowak, M. Matković, M. Radić-Stojković, I. Piantanida, J. Eilmes, Dicationic derivatives of dinaphthotetraaza [14] annulene: synthesis, crystal structures and the preliminary evaluation of their DNA binding properties, Tetrahedron 71(24) (2015) 4163-4173.
[25] I.S. Blagbrough, D. Al-Hadithi, A.J. Geall, Cheno-, urso-and deoxycholic acid spermine conjugates: Relative binding affinities for calf thymus DNA, Tetrahedron 56(21) (2000) 3439-3447.
[26] S. Biswas, S. Samui, A. Chakraborty, S. Biswas, D. De, U. Ghosh, A.K. Das, J. Naskar, Insight into the binding of a non-toxic, self-assembling aromatic tripeptide with ct-DNA: Spectroscopic and viscositic studies, Biochem. Biophys. Rep 11 (2017) 112-118.
[27] J.M. Giulietti, P.M. Tate, A. Cai, B. Cho, S.P. Mulcahy, DNA-binding studies of the natural β-carboline eudistomin U, Bioorganic Med. Chem. Lett. 26(19) (2016) 4705-4708.
[28] K. Karami, F. Parsianrad, M. Alinaghi, Z. Amirghofran, Cyclopalladated complexes containing metformin and benzylamine derivatives: Synthesis, characterization, binding interactions with DNA and BSA, in vitro cytotoxicity studies, Inorg. Chim. Acta 467 (2017) 46-55.
[29] Y.-Y. Lou, K.-L. Zhou, J.-H. Shi, D.-Q. Pan, Characterizing the binding interaction of fungicide boscalid with bovine serum albumin (BSA): A spectroscopic study in combination with molecular docking approach, J. Photochem. Photobiol. B 173 (2017) 589-597.
[30] S. Yasmeen, Exploring thermodynamic parameters and the binding energetic of berberine chloride to bovine serum albumin (BSA): Spectroscopy, isothermal titration calorimetry and molecular docking techniques, Thermochim. Acta (2017).
[31] O.A. Chaves, V.A. da Silva, C.M.R. Sant'Anna, A.B. Ferreira, T.A.N. Ribeiro, M.G. de Carvalho, D. Cesarin-Sobrinho, J.C. Netto-Ferreira, Binding studies of lophirone B with bovine serum albumin (BSA): Combination of spectroscopic and molecular docking techniques, J. Mol. Struct. 1128 (2017) 606-611.
[32] T.F. Cummings, J.R. Shelton, Mannich reaction mechanisms, J. Org. Chem. 25(3) (1960) 419-423.
[33] J.-z. Tian, J.-q. Zhang, X. Shen, H.-x. Zou, Synthesis of phenols and naphthol with n-morpholinomethyl pendants and their dimethylgallium complexes: crystal structure of dimethylgallium-[4-nitro-2-(n-morpholinomethyl)-1-phenoxide], J. Organomet. Chem. 584(2) (1999) 240-245.
[34] K.-W. Chi, Y.S. Ahn, K.T. Shim, T.H. Park, J.S. Ahn, One-pot synthesis of Mannich base using hydroxy aromatic rings and secondary amines, Bull. Korean Chem. Soc. 20 (1999) 973-976.
[35] T. Keleş, B. Barut, Z. Biyiklioglu, A. Özel, A comparative study on DNA/BSA binding, DNA photocleavage and antioxidant activities of water soluble peripherally and non-peripherally tetra-3-pyridin-3-ylpropoxy-substituted Mn (III), Cu (II) phthalocyanines, Dyes Pigm. 139 (2017) 575-586.
[36] N. Shahabadi, M. Maghsudi, Multi-spectroscopic and molecular modeling studies on the interaction of antihypertensive drug; methyldopa with calf thymus DNA, Mol. BioSyst. 10(2) (2014) 338-347.
[37] Y. Li, Z. Yang, M. Zhou, J. He, X. Wang, Y. Wu, Z. Wang, Syntheses, crystal structures and DNA-binding studies of Cu (II) and Zn (II) complexes bearing asymmetrical aroylhydrazone ligand, J. Mol. Struct. 1130 (2017) 818-828.
[38] M.F. Hassan, A. Rauf, Synthesis and multi-spectroscopic DNA binding study of 1, 3, 4-oxadiazole and 1, 3, 4-thiadiazole derivatives of fatty acid, Spectrochim. Acta Part A Mol. Biomol. Spectrosc. 153 (2016) 510-516.
[39] S.R. Wankar, U.J. Pandit, I. Khan, S. Limaye, Photophysical properties and DNA binding studies of novel Eu 3+ mixed ligand complex, J. Lumin. 177 (2016) 416-424.
[40] R. Prabhakaran, P. Kalaivani, P. Poornima, F. Dallemer, R. Huang, V.V. Padma, K. Natarajan, Synthesis, DNA/protein binding and in vitro cytotoxic studies of new palladium metallothiosemicarbazones, Bioorg. Med. Chem. 21(21) (2013) 6742-6752.
[41] S. Murugavel, C.J.P. Stephen, R. Subashini, D. AnanthaKrishnan, Synthesis, structural elucidation, antioxidant, CT-DNA binding and molecular docking studies of novel chloroquinoline derivatives: Promising antioxidant and anti-diabetic agents, J. Photochem. Photobiol. B (2017).
[42] M. Sakthi, A. Ramu, Synthesis, structure, DNA/BSA binding and antibacterial studies of NNO tridentate Schiff base metal complexes, J. Mol. Struct. 1149 (2017) 727-735.
[43] A. Shanmugapriya, G. Kalaiarasi, P. Kalaivani, F. Dallemer, R. Prabhakaran, CT-DNA/BSA protein binding and antioxidant studies of new binuclear Pd (II) complexes and their structural characterisation, Inorg. Chim. Acta 449 (2016) 107-118.
[44] R. Adam, P. Bilbao-Ramos, S. López-Molina, B. Abarca, R. Ballesteros, M.E. González-Rosende, M.A. Dea-Ayuela, G. Alzuet-Piña, Triazolopyridyl ketones as a novel class of antileishmanial agents. DNA binding and BSA interaction, Bioorg. Med. Chem. 22(15) (2014) 4018-4027.
[45] K. Ghosh, S. Rathi, D. Arora, Fluorescence spectral studies on interaction of fluorescent probes with Bovine Serum Albumin (BSA), J. Lumin. 175 (2016) 135-140.
[46] Y.-Y. Lou, K.-L. Zhou, D.-Q. Pan, J.-L. Shen, J.-H. Shi, Spectroscopic and molecular docking approaches for investigating conformation and binding characteristics of clonazepam with bovine serum albumin (BSA), J. Photochem. Photobiol. B 167 (2017) 158-167.
[47] G.-F. Shen, T.-T. Liu, Q. Wang, M. Jiang, J.-H. Shi, Spectroscopic and molecular docking studies of binding interaction of gefitinib, lapatinib and sunitinib with bovine serum albumin (BSA), J. Photochem. Photobiol. B 153 (2015) 380-390.
[48] J.-h. Shi, D.-q. Pan, M. Jiang, T.-T. Liu, Q. Wang, Binding interaction of ramipril with bovine serum albumin (BSA): Insights from multi-spectroscopy and molecular docking methods, J. Photochem. Photobiol. B 164 (2016) 103-111.
[49] M. Anjomshoa, S.J. Fatemi, M. Torkzadeh-Mahani, H. Hadadzadeh, DNA-and BSA-binding studies and anticancer activity against human breast cancer cells (MCF-7) of the zinc

(II) complex coordinated by 5, 6-diphenyl-3-(2-pyridyl)-1, 2, 4-triazine, Spectrochim. Acta Part A Mol. Biomol. Spectrosc. 127 (2014) 511-520.

[50] H. Hadadzadeh, H. Farrokhpour, Z. Jannesari, Z. Amirghofran, Experimental and ONIOM computational evaluation of DNA-and BSA-binding and cytotoxic activity of a mononuclear Pd (II) complex with piroxicam, Inorg. Chim. Acta 453 (2016) 415-429.

[51] K. Liu, H. Yan, G. Chang, Z. Li, M. Niu, M. Hong, Organotin (IV) complexes derived from hydrazone Schiff base: Synthesis, crystal structure, in vitro cytotoxicity and DNA/BSA interactions, Inorg. Chim. Acta 464 (2017) 137-146.

[52] J.-h. Shi, D.-q. Pan, X.-x. Wang, T.-T. Liu, M. Jiang, Q. Wang, Characterizing the binding interaction between antimalarial artemether (AMT) and bovine serum albumin (BSA): Spectroscopic and molecular docking methods, J. Photochem. Photobiol. B 162 (2016) 14-23.

Crystallographic data for the Structures reported in this paper have been deposited with the Cambridge Crystallographic Data Centre (CCDC) as supplementary publication numbers (CCDC 1403704, CCDC 1556655, CCDC 1556656, CCDC 1556657, CCDC 1556658, CCDC 1402257, CCDC 1556659, CCDC 1435610 and CCDC 1570809 for 4a, 4b, 4c, 4d, 4e, 6a, 6b 6d and 6e respectively). Copies of the data can be obtained free of charge from the CCDC (12 Union Road, Cambridge CB2 1EZ, UK; Tel.: + 44-1223-336408;Fax:+44-1223-336003;e-mail: deposit@ccdc.cam.ac.uk;Website http://www.ccdc.cam.ac.uk).

Supplementary Material

FTIR, ^{1}H NMR, ^{13}C NMR, and Mass spectrum for all the compounds and ORTEP of 4b, 4c, 4d, 4e, 6b, 6d, 6e and 6f and their crystal data .

The CT DNA and BSA binding studies UV visible, emission and synchronous fluorescence spectra of 4b, 4c, 4d, 4e, 6b, 6d , 6e and 6f.

Highlights

- Amino aryl methylated paracetamol derivatives were synthesized.
- One pot, non-catalysed and simple MCR gave good yield.
- Solid state structures of the compounds were studied using single crystal X-ray diffraction studies.
- Evaluation of CT DNA and BSA binding properties by spectroscopic methods.

Declaration of interestsV

☐ **V** The authors declare that they have no known competing financial interests or personal relationships that could have appeared to influence the work reported in this paper.

☒The authors declare the following financial interests/personal relationships which may be considered as potential competing interests:

√ The authors declare that they have no known competing financial interests or personal relationships that could have appeared to influence the work reported in this paper.